HHS Public Access

Author manuscript

Kidney Int. Author manuscript; available in PMC 2014 November 01.

Published in final edited form as:

Kidney Int. 2014 May ; 85(5): 1078–1090. doi:10.1038/ki.2013.456.

Peripheral blood CD8αα⁺CD11c⁺MHC⁻II⁺CD3- cells attenuate autoimmune glomerulonephritis in rats

Jean Wu, BS, **Cindy Zhou, MD, Ph.D.**[1], **Julie Robertson, Ph.D.**[2], **Colin Carlock, BS**, and **Yahuan Lou, Ph.D.**

Department of Diagnostic and Biomedical Sciences, SD, University of Texas Health Science Center at Houston, Houston, TX 77054

Abstract

In an anti-GBM glomerulonephritis (GN) model, GN-resistant Lewis rats naturally recover from early glomerular inflammation. Here we investigated recovery mechanisms for development of a potential immunotherapy for autoimmune GN. Our previous studies suggested that glomeruli-infiltrating leukocytes with a phenotype of CD8αα$^+$CD11c$^+$MHC$^-$II$^+$CD3$^-$ (GIL CD8αα$^+$ cells) were responsible for recovery through induction of T cell apoptosis. Now, we identified peripheral blood CD8αα$^+$CD11c$^+$MHC$^-$II$^+$CD3$^-$ cells (PBMC CD8αα$^+$CD3$^-$ cells), which shared 9 markers with GIL CD8αα$^+$ cells. Upon incubation, PBMC CD8αα$^+$CD3$^-$ cells displayed a morphology resembling that of dendritic cells. Similar to GIL CD8αα$^+$ cells, PBMC CD8αα$^+$CD3$^-$ cells were capable of inducing T cell apoptosis *in vitro*. Hence, PBMC CD8αα$^+$CD3$^-$ cells were likely the precursor of GIL CD8αα$^+$ cells. We next tested their potential *in vivo* function. PBMC CD8αα$^+$CD3$^-$ cells were able to infiltrate inflamed but not normal glomeruli. Isolated PBMC CD8αα$^+$CD3$^-$ cells of Lewis rats were transferred into GN-prone Wistar Kyoto rats at early inflammatory stage (day 17–25). When examined at day 45, both histopathology and BUN/serum creatinine level showed significantly attenuated GN in 80% of cell recipient Wistar Kyoto rats. Separate experiments verified infiltration of transferred Lewis PBMC CD8αα$^+$CD3$^-$ into the glomeruli, accompanied with apoptotic CD4$^+$ T cells in the glomeruli of the recipient Wistar Kyoto rats. Thus, PBMC CD8αα$^+$CD3$^-$ cells of Lewis rats were able to terminate ongoing autoimmune inflammation in the glomeruli.

INTRODUCTION

Traditional treatments of inflammatory kidney diseases including anti-GBM glomerulonephritis (GN) are largely based on anti-inflammatory chemotherapies.[1] Developing novel therapies for inflammatory diseases is a clinical priority. Cell-based immunotherapy is a promising strategy for treating various human inflammatory

Correspondence: Dr. Ya-Huan Lou, Department of Diagnostic Sciences, DB, University of Texas Health Science Center at Houston, Houston, TX 77054, Phone: 713-486-4059, Fax: 713-486-0540, Yahuan.Lou@uth.tmc.EDU.

[1]Current Address: Department of Diagnostic Oncology, University of Maryland, Baltimore, MD21201

[2]Current Address: Clinical Immunology, Oklahoma Medical Research Foundation, Oklahoma City, OK 73104

DISCLOSURES

None

diseases.[2–4] However, immune cells which can specifically silence an inflammation must be identified before developing such therapies.[4]

Regulatory/tolerogenic dendritic cells (DCs) have been considered for immunotherapies for inflammatory autoimmune diseases.[5–8] These cells reside in lymphoid organs and eliminate naive self-reactive T cells by inducing apoptosis or skewing their differentiation into regulatory T cells. Thus, autoimmunity is prevented *de novo*. However, those mechanisms are not effective if naive autoreactive T cells have been accidentally activated and are causing tissue inflammation.[9, 10] Other mechanisms must exist to terminate the inflammation in the target tissues. Discovering such mechanisms will be more relevant to the development of novel immunotherapies for an existing autoimmune GN.

We have developed a rat model for anti-GBM GN, which is induced by T cell epitope pCol(28–40) of the autoantigen collagen 4α3 chain.[11–13] GN-prone Wistar Kyoto (WKY) rats develop severe glomerular inflammation, which is eventually terminated and replaced by progressive fibrosis.[13] In spite of sharing identical MHC and mounting a similar T cell response to WKY rats, the Lewis (LEW) strain is GN-resistant.[14] The GN-resistance in LEW is due to a spontaneous termination of T cell-mediated GN at an early stage.[14] We have identified a $CD8\alpha\alpha^+CD11c^+MHC\text{-}II^+CD3^-$ population among glomeruli-infiltrating leukocytes (designated as GIL $CD8\alpha\alpha^+$ cells), which was able to induce T cell apoptosis.[15] Interestingly, the cell's invasion of glomeruli was also closely associated with termination of inflammation and T cell apoptosis in the glomeruli during recovery in LEW rats.[16] The present study aimed to identify the precursor of GIL $CD8\alpha\alpha^+$ cells in peripheral blood mononuclear cells (PBMC), and to test if this population was able to inhibit glomerular inflammation.

RESULTS

Identification of PBMC $CD8\alpha^+RT1.B^+$ $CD11^{low}$ $CD3^-CD94^-$ cells

GIL $CD8\alpha\alpha^+$ cells are derived from bone marrow, suggesting that the cells migrate into inflamed glomeruli through peripheral blood.[15] We first searched for $CD8\alpha^+CD3^-$ non-T cells among peripheral blood mononuclear cells (PBMC) in LEW rats. A $CD8\alpha^+CD3^-$ population (approximately 2.9% of PBMC) was observed (Figure 1a). Another analysis showed a $CD8\alpha^+RT1B(MHC\text{-}II)^+$ of a similar size (2.7%)(Figure 1b). Because $CD8^+$ T cells do not express MHC-II, the above $CD8\alpha^+CD3^-$ population was determined to be $RT1B^+$. Next, we sorted whole PBMC $CD8\alpha^+$ cells (both $CD3^+$ and $CD3^-$). Based on the FSC and SSC plot of flow cytometry, $CD8\alpha^+CD3^-$ cells formed a cluster, which was distinguishable from $CD8^+$ T cells (Figure 1c). A previous study has reported $CD8^+$ regulatory T cells in a LEW rat model for Heymann nephritis.[17] Thus, we further tested the above PBMC $CD8\alpha^+$ cells for their CD8β and CD3 expression using three color flow cytometry. The PBMC $CD8\alpha^+$ cells contained two distinct populations: $CD8\alpha^+\beta^+CD3^+$ T cells and $CD8\alpha^+\beta^-CD3^-$ non-T cells (Figure 1d). Since the $CD8\alpha^+\beta^-CD3^-$ cell population did not express CD8β, they were designated as PBMC $CD8\alpha\alpha^+CD3^-$ cells. A subset of NK cells is $CD8^+$. Using CD94 as an NK marker, we showed that the majority of $CD94^+$ NK cells were $CD8\alpha^-$ with a minor $CD94^+CD8\alpha^+$ population, which was approximately 0.7% of total PBMC (Figure 1e). Thus, the $CD94^+CD8\alpha^+$ NK cells could be a small portion, but

not all of the CD8αα$^+$CD3$^-$cells. In summary, our preliminary observations of PBMC suggested that there was a CD8αα$^+$RT1.B$^+$CD3$^-$CD94$^-$CD3$^-$ non-NK non-T cell population among PBMC, which formed a morphologically identical population. However, this was not conclusive. Therefore, we purified this population for further characterization.

We compared PBMC CD8αα$^+$CD3$^-$ populations between normal and immunized rats. This population significantly expanded in the rats, which had been immunized 20 ds previously (Figure 1f). The population CD8αα$^+$CD3$^-$ accounted for 2.9–3.3% of PMBC in the un-immunized rats, as compared to up to 7–15% in the immunized rats. In all the following experiments, immunized LEW rats were used for studying PBMC CD8αα$^+$CD3$^-$ cells.

Characterization of purified PBMC CD8αα$^+$CD3$^-$ cells

PBMC CD8αα$^+$CD3$^-$ cells were purified for further characterization. The purified cells formed a morphologically unique population with 93±2% to be CD8α$^+$CD3$^-$ based on 5 experiments (Figures 2a and b). The PBMC CD8αα$^+$CD3$^-$ cells expressed CD11c and various level of RT1B (MHC class II) (Figures 2c and d). In general, RT1B expression level was lower than that of GIL CD8αα$^+$ cells (Figure 2e). The PBMC CD8αα$^+$CD3$^-$ cells did not express CD94, TcRγδ (a marker for γδT cell), CD68 (ED1, a marker for monocyte and phagocyte subsets), and α2E integrin (OX62, a marker for subsets of rat DCs in lymphoid tissues)[18] (Figure 2g). The cells were further characterized by RT-PCR for additional DC markers due to a lack of antibodies. RT-PCR showed that PBMC CD8αα$^+$CD3$^-$ cells expressed CD14, CD83 and CCR7 but not TLR3 or OX40L (Figure 2f). The expression pattern of these markers was nearly identical between PBMC CD8αα$^+$CD3$^-$ and GIL CD8αα$^+$ cells (Table 1).

The PBMC CD8αα$^+$CD3$^-$ cells' morphology was examined. Immunofluorescence confirmed co-expression of cell surface RT1B and CD8α in those cells (Figure 2h). The PBMC CD8αα$^+$CD3$^-$ cells had a polygonic nucleus, in contrast to a kidney-shaped nucleus in monocytes (Figure 2h). They could also be easily distinguished from CD8$^+$ T cells or NK cells by either their size or shape (Figure 2h). Morphological changes in PBMC CD8αα$^+$CD3$^-$ cells, along with both surface and intracellular MHC-II expression, were observed after *in vitro* culture in comparison to monocytes. Freshly isolated PBMC CD8αα$^+$CD3$^-$ cells were spherical. Many cells flattened after 12–36 hrs' culture, and became irregularly shaped with various cellular projections at 60 hrs (Figure 3a). Staining with CD8α antibody revealed fine cellular projections in majority of cells, which resembled those of DCs (Figure 3b), suggesting that PBMC CD8αα$^+$ cells were a type of phagocyte. On the other hand, most monocytes remained spherically shaped at 36 hrs (Figure 3c).

We next examined if LPS would stimulate MHC class II expression in the cultured PBMC CD8αα$^+$CD3$^-$ cells. Nephritogenic T cell epitope is restricted by MHC-II RT1D^l.[12] Thus, we examined the cells' expression of RT1D. First, expression of RT1D in freshly purified PBMC CD8αα$^+$CD3$^-$ cells was confirmed at the protein level by immunofluorescence and western blot (Figure 3d). Intracellular RT1D was also detectable in the cells after permeablization (Figure 3e). Using the Golgi block method for 6 hrs, we observed a detectable increase in intracellular RT1D, suggesting active synthesis of MHC class II molecules (Figure 3f). Flow cytometry showed that the majority of freshly purified PBMC

CD8αα$^+$CD3$^-$ cells expressed a low level of surface RT1D (d0), with a minor subset expressing mid-level RT1D (Figure 3g). Surface RT1D levels rapidly increased at d1 with the majority of the cells expressing mid-level of RT1D (Figure 3g). At d3, a small portion of the cells showed high levels of RT1D, although most of the cells still remained unchanged (Figure 3g).

PBMC CD8αα$^+$CD3$^-$ cells induce T cell apoptosis

We have previously shown that GIL CD8αα$^+$ cells are able to induce T cell apoptosis.[15] We tested whether the PBMC CD8αα$^+$CD3$^-$ cells had a similar ability. Isolated PBMC CD8αα$^+$CD3$^-$ cells were co-incubated with resting pCol(28–40)-specific T cells from two independent cell lines in the presence of 10 mM pCol(28–40). As controls, T cells were incubated with thymic antigen presenting cells (APCs), PBMC CD8α$^-$ cells (mainly monocytes), or GIL CD8αα$^+$ cells under the same conditions. T cells alone served as another control. Incubation with thymic APCs led to T cells to proliferate after 36 hrs.[12] T cells incubated with PBMC CD8α$^-$ monocytes showed much less signs of T cell proliferation, but no T cell death (Figure 4a). However, incubation with PBMC CD8αα$^+$CD3$^-$ cells or GIL CD8αα$^+$ cells led to significant T cell death after 24–36 hrs, evidenced by the presence of fewer T cells and numerous cellular debris. Almost no living T cells were present in the incubation after d3 (Figure 4a). DNA fragmentation assays were performed using DNA isolated from various incubations at d1 and d2. No DNA fragmentation was detected in T cells alone or T cells incubated with thymic APCs at both days (Figure 4b). In contrast, DNA fragmentation could be observed in the incubation with PBMC CD8αα$^+$CD3$^-$ cells at d1 and became highly significant at d2, which was comparable to that of incubation with GIL CD8αα$^+$ cells (Figure 4b).

Two methods confirmed apoptosis in the T cells. The cells were harvested at 36 hrs. Because PBMC CD8αα$^+$CD3$^-$ cells adhered to the plate, only non-adhesive T cells and cellular debris were harvested (see Figure 4a). *First*, the cells were co-stained with TUNEL and CD4 antibody. Flow cytometry showed 26% of CD4$^+$ cells to be TUNEL$^+$ in the incubation with PBMC CD8αα$^+$CD3$^-$ (Figure 4c). Although there were only a few T cells left, 87% of CD4$^+$ cells were TUNEL$^+$ at d3 (Figure 4c). Immunofluorescence confirmed the nuclear staining for TUNEL in many CD4$^+$ cells (Figure 4e). In contrast, the incubation with PMBC CD8α$^-$ showed only an insignificant number (<3%) of cells to be TUNEL$^+$CD4$^+$ (Figure 4c). *Second*, apoptosis in T cells was analyzed by co-staining with annexin V and CD3 or CD4 antibodies. Approximately 31% of CD4$^+$ cells were annexin$^+$ after 36 hrs incubation (Figure 4d). Immunofluorescence revealed surface annexin V in CD3$^+$ cells (Figure 4f). In contrast, incubation with PMBC CD8α$^-$ monocytes did not lead to a significant CD4$^+$annexin V$^+$ cell population (Figure 4d). Thus, similar to GIL CD8αα$^+$ cells, PBMC CD8αα$^+$CD3$^-$ cells were able to induce T cell apoptosis.

PBMC CD8αα$^+$CD3$^-$ cells are able to infiltrate inflamed glomeruli

In vitro migration assays were first performed to test whether the PBMC CD8αα$^+$CD3$^-$ cells migrated toward inflamed glomeruli. Normal or inflamed glomeruli were isolated from immunized WKY rats at d0 and d30. PBMC CD8αα$^+$CD3$^-$ cells were isolated from immunized LEW rats at d20, labeled with CFSE, and used as probes. After 14-hr incubation,

the number of the PBMC CD8αα$^+$CD3$^-$ cells which had migrated toward inflamed glomeruli was 13–15 folds as many as those which migrated toward normal glomeruli (Figure 5a). However, this result did not rule out the possibility that the migration was non-specific as only PBMC CD8αα$^+$ cells were tested. Next, the whole PBMC CD8$^+$ population (both CD3$^+$ and CD3$^-$) was used. Approximately 9% of the cells migrated toward inflamed glomeruli. Among the migrated CFSE$^+$ PBMC CD8$^+$ cells, RT1B$^+$ cells were enriched by 4-fold (from 14% to 54%)(Figure 5b). Approximately 1% of the cells had migrated to the normal glomeruli; flow cytometry showed only 11.7% of the migrated cells were RT1B$^+$ cells (Figure 5b). Thus, the absolute number of migrated CD8α$^+$RT1B$^+$ cells toward inflamed tissue was approximately 35 fold over those toward the normal glomeruli, suggesting the migration of CD8αα$^+$CD3$^-$RT1B$^+$ cells toward inflamed tissue to be specific. With similar methods, immunized GFP-Tg LEW rats were used as PBMC CD8αα$^+$CD3$^-$ cell donors. The number of GFP$^+$ PBMC CD8αα$^+$CD3$^-$ cells, which migrated toward inflamed glomeruli, was 7 fold great than those which had migrated toward normal glomeruli. When whole PBMC CD8$^+$ cells (both CD3$^+$ and CD3$^-$) from immunized GFP Tg rats were used, flow cytometry analysis showed that 38% of the GFP$^+$ cells, which migrated toward inflamed glomeruli, were RT1B$^+$, in contrast to only 5.9% cells which migrated toward normal glomeruli (Figure 5c). This experiment again showed the migration was specific.

We next tested whether PBMC CD8αα$^+$ cells were able to migrate into inflamed glomeruli *in vivo*. CFSE-labeled PBMC CD8αα$^+$CD3$^-$ cells of immunized LEW rats were transferred into normal WKY rats or those which had been immunized with pCol(28–40) 35 days previously (three rats/group). The cell recipients were sacrificed after 24 hr. In normal WKY rats, a few labeled cells were observed in the interstitial tissue, but none of them were found in the glomeruli. However, a significant number of labeled PBMC CD8αα$^+$CD3$^-$ cells were observed in both interstitial tissue and the glomeruli of immunized recipients (Figure 5d). Labeled PBMC CD8αα$^+$ cells were observed to be among other inflammatory cells, including endogenous tissue CD8αα$^+$ cells (Figure 5e). Importantly, over 60% of the labeled cells were located in the glomeruli (Table 2). Statistical analysis on distribution preference (glomeruli vs interstitial tissue) demonstrated that accumulation of the labeled cells in glomeruli was highly specific ($p<0.0001$)(Table 2). Next, PBMC CD8αα$^+$CD3$^-$ cells of immunized GFP-Tg LEW rats were used for transfer. Due to the availability of GFP-Tg LEW rats, only 1 million PBMC CD8αα$^+$GFP$^+$ cells were injected into immunized or normal WKY rats (two rats/group). This yielded a similar result (Figure 5f). A small CD8α$^+$GFP$^+$ population was detectable among isolated glomerular cells (Figure 5g). Thus, both *in vitro* and *in vivo* experiments showed that PBMC CD8αα$^+$CD3$^-$ cells from immunized LEW rats were able to infiltrate inflamed glomeruli *in vivo*.

Transferring PBMC CD8αα$^+$CD3$^-$ cells of LEW rats attenuates GN in recipient WKY rats

The above observations suggested that PBMC CD8αα$^+$CD3$^-$ cells were the precursors of GIL CD8αα$^+$ cells. We questioned if transferring PBMC CD8αα$^+$CD3$^-$ cells of LEW origin would infiltrate inflamed glomeruli earlier to terminate an on-going inflammation in GN-prone WKY rats. Immunized WKY rats usually develop T cell-mediated glomerular inflammation at d17.[13, 14] PBMC CD8αα$^+$CD3$^-$ cells of immunized LEW rats were

transferred into the immunized WKY rats at d17, 20 and 25. As a transfer control, five immunized WKY rats were transferred with PBMC $CD8^-$ monocytes. Another five immunized WKY rats did not receive any cell transfers for monitoring GN development. When observed at d45, significantly reduced disease severities were observed in 8 out of 11 PBMC $CD8\alpha\alpha^+$ cell recipients (Figure 6a and d). Two recipients were almost free of inflammation, while the other 6 only showed a mild inflammation or leukocyte infiltration. It is worthwhile to note that the glomeruli were slightly dilated in these rats with mild inflammation or without inflammation (Figure 6d). Dilation of glomeruli has been observed in the recovered LEW rats.[16] The remaining three recipients developed significant inflammation with one having mild fibrosis. In contrast, five $CD8^-$ cell recipients and four immunized rats without cell transfer developed ascites. Two rats from each control died before the end of the experiments. Severe fibrosis was observed in all control rats except one (Figure 6a). Circumferential fibrous crescents and segmental necrosis were often observed in those control rats (Figure 6d and f). The above results suggested that those control rats developed end stage renal disease. This was supported by the elevated BUN and serum creatinine in the survival control rats (Figure 6b and c). On the other hand, BUN and serum creatinine levels in the PBMC $CD8\alpha\alpha^+CD3^-$ cells recipients were significantly lower than those of the two controls, though they were slightly higher than those in CFA immunized rats (Figure 6b and c). Next, immunofluorescence was used to evaluate glomerular inflammation. Immunized WKY rats usually show accumulation of $ED1^+$ macrophages and other leukocytes in their glomeruli with GBM-bound IgG antibodies at d25 post immunization (Figure 6e).[11] At d45, intense GBM-bound IgG antibodies were detectable before tufts completely collapsed in immunized WKY rats, but inflammatory cells such as $ED1^+$ cells are no longer present.[11] This was exactly observed in the two control groups (Figure 6f). On the other hand, almost half of PBMC $CD8\alpha\alpha^+CD3^-$ recipient WKY rats showed no or a few $ED1^+$ cells in their glomeruli at d45 (Figure 6f). However, a low level of GBM-bound IgG antibodies was observed in PBMC $CD8\alpha\alpha^+CD3^-$ recipients even without significant inflammation (Figure 6f). Presence of GMB-bound IgG antibodies suggests pre-existing glomerular inflammation in the recipients before PBMC $CD8\alpha\alpha^+CD3^-$ cell transfers.

In two other experiments, three immunized WKY rats each were transferred with the PBMC $CD8\alpha\alpha^+CD3^-$ cells of LEW rats at d17 and 20; three other immunized WKY rats without transfer served as a positive control. The cell recipients or controls were sacrificed at d23. In the first experiment, immunofluorescence showed a significant increase in GIL $CD8\alpha\alpha^+$ cells in the cell recipients as compared to the controls (Figure 7a and b). The recipients also showed a slightly lower number (though not significantly different) of $ED1^+$ macrophages in the glomeruli than those in the immunized controls (Figure 7b). In the second experiment, glomerular T cells and GIL $CD8\alpha\alpha^+$ cells were isolated for genotyping (Figure 7c). Due to a low number, glomeruli-infiltrating pan-T cells and GIL $CD8\alpha\alpha^+$ isolated from the three cell recipients were pooled. PCR genotyping using three polymorphic DNA microsatellites showed that the majority of the isolated GIL $CD8\alpha\alpha^+$ cells were of LEW origin, while $CD3^+$ T cells were of WKY origin (Figure 7c). This experiment was repeated once and a similar result was yielded. T cells from the controls were of WKY origin. We failed to yield sufficient GIL $CD8\alpha\alpha^+$ cells for analysis due to their low number at d23.[16] A portion of

glomerular T cells were used to test if they were undergoing apoptosis (Figure 7c). After incubation for one day, apoptosis in $CD3^+$ T cells was determined. First, DNA fragmentation assay showed apoptotic T cells in PBMC $CD8\alpha\alpha^+CD3^-$ cell recipient WKY rats, but not in the immunized controls (Figure 7d). Flow cytometry after TUNEL staining confirmed that about 41% of $CD3^+$ T cells were apoptotic in PBMC $CD8\alpha\alpha^+CD3^-$ cell recipients, as compared to less than 5% in immunized WKY control (Figure 7e). Finally, renal sections from PBMC $CD8\alpha\alpha^+CD3^-$ cell recipients or immunized controls were stained for caspase 3 using the immunoperoxidase method.[16] PBMC $CD8\alpha\alpha^+CD3^-$ cell recipients showed clustered caspase 3^+ cells in their glomeruli (Figure 7f), which was similar to those observed in LEW rats during recovery at d23.[16] As expected, no caspase 3^+ cells were observed in the immunized WKY rats at d23 (Figure 7f).

DISCUSSION

We have previously identified a $CD8\alpha\alpha^+CD11b/c^+MHC^+OX62^-$ DC-like population (GIL $CD8\alpha\alpha^+$ cell). The cells actively infiltrate glomeruli during the transition stage from severe inflammation to fibrosis, and induce T cell apoptosis through antigen presentation *in vitro*.[15] These results suggested that the cells may terminate glomerular inflammation *in vivo* prior to fibrosis. Furthermore, we have shown that GN-resistant LEW rats naturally recover from early glomerular inflammation,[14] and that the recovery is also closely associated with invasion of GIL $CD8\alpha\alpha^+$ and T cell apoptosis.[16] These results again supported that GIL $CD8\alpha\alpha^+$ cells may have terminated inflammation. Seemingly paradoxical consequences of GIL $CD8\alpha\alpha^+$ cell's infiltration in GN-resistant and –prone rats may depend on the timing of infiltration (Figure 8). Infiltration at early stages of inflammation leads to healing or recovery, while infiltration after inflammation advances only leads to a pathological healing process, fibrosis (Figure 8). However, this mechanism is one among many others, which contribute to GN susceptibility. This issue will be discussed later. In the present study, we identified a PBMC $CD8\alpha\alpha^+$ population which was the precursor of GIL $CD8\alpha\alpha^+$ cells; the transfer of these PBMC $CD8\alpha\alpha^+$ cells into GN-prone WKY rats at the early stages of the disease led to significantly attenuated GN. The cell transfer experiments provided us direct evidence supporting our hypothesis that this novel $CD8\alpha\alpha^+$ population is involved in termination of an existing autoimmune inflammation in the target tissue.

Although anti-GBM GN in our model is induced by a well characterized T cell mechanism, anti-GBM antibodies to diverse GBM autoantigens are produced at late stages post glomerular injury through B cell epitope spreading mechanism. Those autoantibodies are most likely not involved in initiation of the disease. However, it remains unknown if they play any roles in anti-GBM GN pathogenesis. In this study, inhibition of T cell mediated glomerular injury by transferring PBMC $CD8\alpha\alpha^+CD3^-$ cells led to attenuated GN. However, a reduced amount of anti-GBM antibodies were still detectable in the cell recipients. We don't know the origin of those antibodies. It is possible that PBMC $CD8\alpha\alpha^+CD3^-$ cells may induce T cell apoptosis only in the inflamed glomeruli, but not in the renal draining lymph nodes where autoantibodies were originated. This may provide an opportunity to look at role of those autoantibodies.

The present study suggested PBMC CD8αα$^+$ cells to be the precursors of GIL CD8αα$^+$ cells through the comparison of phenotype, morphology and functions between the two. Both GIL CD8αα$^+$ and PBMC CD8αα$^+$CD3$^-$ cells were CD8αα$^+$CD11c$^+$MHC II$^+$ with expression of almost identical other markers for DCs. Functionally, both were able to infiltrate inflamed glomeruli and induce T cell apoptosis. The GIL CD8αα$^+$ cells are derived from bone marrow.[15] Thus, the lineage of these CD8αα$^+$ cells can be summarized as follows: 1) an unidentified bone marrow progenitor, 2) circulating PBMC CD8αα$^+$CD3$^-$ cells, and 3) GIL CD8αα$^+$ cells. It is worthwhile to mention the expansion of the PBMC CD8αα$^+$CD3$^-$ cells after immunization. However, it remains unclear how this population expands and why. The following questions need to be addressed. *First*, whether is the expansion a response to immunization or specifically to autoimmunity? *Second*, whether the expansion is induced by CFA alone, any types of antigens, or only to autoanitgens? *Third*, whether PBMC CD8αα$^+$ cells in GN-resistant LEW rats and GNprone WKY rats expand at different times post immunization which leads to opposite consequences? *Finally*, we need to confirm if CD8αα$^+$CD3$^-$ population in immunized and non-immunized animals are identical. We should also identify what factor(s) initiate their expansion.

We believe that the PBMC CD8αα$^+$CD3$^-$ cells are a type of dendritic cells (DC), which possess a capacity in induction of T cell apoptosis.[19–22] Using various markers, DCs in the kidney have been investigated in detail especially in mice.[23–26] Similar to other tissues, at least three subsets of conventional and plasmacytoid DCs have been found in normal kidneys. A subset of conventional DCs of myeloid origin with a phenotype of CD4$^+$CD11c$^+$CX3CR1$^+$ is dominant and probably constitutes an immune surveillance network.[25] None of these kidney DCs are present within glomeruli, although they may surround the glomeruli. In addition, renal interstitial tissues, but not glomeruli, contain a small number of CD8$^+$ lymphoid DCs.[23, 26] Thus, it is unlikely that GIL CD8αα$^+$ cells are the same cells of these previously described DCs in normal kidneys, because these DCs are present only in the interstitial tissues. DCs in autoimmune or inflammatory kidney diseases have also been investigated.[26–30] CD11c$^+$ DCs have been located in interstitial or periglomerular areas in a murine inflammatory glomerulonephritis model.[27] Depletion of these CD11c$^+$ DCs attenuated GN, suggesting a critical role of DCs in the maintenance of glomerular inflammation.[28] Several studies have suggested DCs' roles in both promotion and inhibition of autoimmunity in murine lupus nephritis.[29, 30] However, more detailed characterization of the above DCs are needed for comparison to our PBMC CD8αα$^+$ cells.

The transfer of PBMC CD8αα$^+$CD3$^-$ cells attenuated GN severity in GN-prone WKY rats. However, a previous study showed that depletion of CD8$^+$ cells prevented GN in WKY in another model.[31] There are several explanations. *First*, GN-causing mechanisms may be different in the two models. GN in our model is induced by a well characterized autoreactive T cell mechanism.[11–13] Second, *in vivo* depletion would lead to eliminate all CD8 bearing leukocytes such as other CD8$^+$ DCs/macrophages, T cells and NK cell. Thus, it is unclear if a group of CD8$^+$ such as T cells, which play a positive role in GN pathogenesis, could also be eliminated. Our preliminary study showed that *in vivo* depletion of CD8$^+$ cells in LEW rats greatly affected T cell response to the immunization for unknown reasons.

By mimicking this mechanism, we may provide a concept for a potential cellular immunotherapeutic strategy for termination of early, but not late stage, GN. It is technically feasible to genetically modify PMBC CD8αα$^+$ cells of a patient to promote the cell's expansion and/or infiltration of the inflamed autoimmune target tissue. However, there are several issues to be addressed before development of this concept. First, in humans, no DC subsets express CD8αα. Thus, we need to determine if a similar population exists in humans.[32] A recent study has reported a human DC subset in the spleen, which did not express CD8αα, but has a similar function as the rodents CD8$^+$ DCs.[33] It is unclear, however, if this population represents other CD8$^+$ like DCs in human. Second, we need to examine the infiltration of a similar DC in inflamed glomeruli in humans. However, it seems difficult since human DC lacks CD8 expression. It is necessary to emphasize that our finding may represent only one new mechanism among many others for prevention or inhibition of autoimmune diseases. These mechanisms may complement each other or function at different levels. In anti-GBM disease models, multiple such mechanisms have been described. A novel CD8$^+$ regulatory T cell has been reported to be critical in controlling anti-GBM disease in a rat model.[17] Involvement of cytokines such as TGF-β released by regulatory T cells has been well studied in anti-GBM disease.[34, 35] Genetic studies have linked copy number of the Fcγ receptor encoding gene to anti-GBM GN in a rat model.[36] Because Fcγ receptor is widely expressed in various antigen presenting cells such as macrophages and dendritic cells, it will be very interesting to compare its expression level in PBMC CD8αα$^+$CD3$^-$ cells or other phagocytes between WKY and LEW rat. In addition, the role of apoptosis in crescentic GN is still largely unclear. Thus, it needs to be determined if T cell apoptosis is involved in susceptibility in human crescent GN.

MATERIALS AND METHODS

Antibodies

Biotin labeled anti-rat CD3 (G.4.18), PE-labeled anti-rat CD4 (OX35), CD8α (OX8), CD11c, RT-1B (OX6), FITC labeled anti-rat CD8α, RT-1B (OX6), RT-1D (OX17), OX62, TcRγδ, CD11b and α2E integrin (OX62), and APC-labeled CD8α were from Pharmingen (San Diego, CA). FITC-labeled anti-rat CD8β, biotin labeled rabbit anti-rat caspase 3 antibody (D175) were from Cell Signaling Technologies. Goat anti-CD34, CD94 and TLR3, and antibodies to CD68 (ED1) and rat NK marker (ANK61) were from Santa Cruz. Anti-rat CD32 (D34-485) was used for Fc block. PE, FITC, or HRP-labeled anti-rat IgG, and purified rat IgG were from Southern Biotechnology (Birmingham, AL). Various mouse Ig isotypes (BD Biosciences, San Diego, CA) and normal rat/mouse IgG (Southern Biotechnology) were used as controls in both flow cytometry and immunofluorescence.

Induction and evaluation of glomerulonephritis

All procedures involving animals in this study were approved by the institutional animal welfare committee. Female WKY or LEW rats (4–6 weeks of age) were purchased from Harlan (Indianapolis, IN). Female LEW-Tg (EGFP) F455/Rrrc rats (LEW GFP-Tg), in which only BM-derived cells expressed various levels of GFP, were provided by the University of Missouri, MO. Rats were immunized with peptide pCol(28–40) (0.15 μmol) emulsified in CFA, in one hind footpad and at the base of the tail.[13] GN was evaluated by

albuminuria and renal histopathology. Renal tissues fixed in Bouin's fixative were used for H&E staining, or fixed in 4% paraformaldehyde (PFA) for immunochemical staining. A combination of H-E staining and immunofluorescence for $ED1^+$ and $CD4^+$ cells allowed us to give each glomerulus a score: 0 (normal) 1 (leukocyte infiltration) 2 (mild inflammation) 3 (inflammation) and 4 (fibrosis). Leukocyte infiltration indicated increased intra- or peri-glomerular $CD4^+$ and $ED1^+$ cells detected by immunofluorescence. For glomerular inflammation, clustered mononuclear leukocytes with significant structural changes such as dilation of glomeruli were detectable on H-E staining. Sub-score for each score group was first calculated (= glomeruli number×score). Severity of GN in a rat was expressed as glomeruli injury scores (GIS) based on > 100 glomeruli. GIS = sum of sub-scores ÷ total glomeruli number. In Addition, BUN and serum creatinine were measured with two commercial kits from Arbor Assay (Ann Arbor, MI) and Cayman Chem. (Ann Arbor, MI), respectively.

Detection of Apoptotic T Cells

Staining of TUNEL and annexin V (Apoptosis detection kit, BioVision, Mountain View, CA), together with CD4 or CD3 antibody, were utilized to detect apoptotic T cells *in vitro*, followed by flow cytometry or fluorescent microscopy. Immunoperoxidase was performed to detect apoptotic T cells in glomeruli using an antibody to caspase 3.[16] DNA fragmentation test was also utilized to detect apoptosis using the Apoptotic-LADDER™ kit (G-Bioscience, ST. Louis, MO).

In vitro migration assays

Glomeruli were isolated from WKY rats at d35 post immunization following a previously published method.[15] Glomeruli (5×10^4) were placed in the lower compartment of the Transwell® system (Corning Lowell, MA). At the same time, total PBMC $CD8\alpha^+$ cells or $CD8\alpha\alpha^+CD3^-$ subsets were isolated from immunized LEW rats or EGFP-Tg LEW rats and placed (10^6 cells) in duplicate in the Transwell insert (Φ6.5mm with pore size 3.0μm). Glomeruli isolated from normal rats served as a control. As additional controls, some wells only contained PBMC $CD8\alpha\alpha^+CD3^-$ cells in the insert or only glomeruli in the lower compartments. The assembled Transwells were incubated at 37oC with 5% CO_2 for 14 hours. The cells were harvested from the lower compartments and counted. In some cases, PBMC $CD8\alpha\alpha^+CD3^-$ cells were first labeled by CFSE before the assay.[12] Migrated cells from the lower compartments were analyzed with flow cytometry or other methods.

PBMC $CD8\alpha\alpha^+CD3^-$ cell purification, labeling and transfer

PBMC fractions were first isolated from immunized LEW rats by Ficoll gradient centrifugation. Whole PBMC $CD8\alpha^+$ cells, which included both $CD8^+CD3^+$ and $CD8^+CD3^-$ cells, were positively isolated by a CD8α antibody with a cell sorter as described above. For isolation of PBMC $CD8\alpha\alpha^+CD3^-$ cells, T cells were first positively removed from PBMC by a pan-T cell isolation kit (Miltenyi Biotec, Germany), followed by positive $CD8\alpha^+$ cell sorting. For labeling experiments, freshly isolated PBMC $CD8\alpha\alpha^+CD3^-$ cells were washed with HBSS, adjusted to 10^7cells/ml, and labeled by CFSE (Molecular Probes, Eugene, OR) following a published method.[15] The labeled cells

(2×10^6cells/rat) were injected into untreated or immunized rats. In some cases, PBMC CD8αα$^+$CD3$^-$ cells were isolated from EGFP-Tg LEW rats for transfer. The cell recipients were sacrificed 24 hours after the cell transfer. Different organs including lung, liver, pancreas, spleen, lymph nodes, and kidney were removed and either fixed in 3% PFA or snap-frozen. Serial frozen sections (3 μm) which cut through 10 glomeruli were used for counting labeled cells. The labeled cells in the glomeruli or interstitial tissue were counted separately. For testing PBMC CD8αα$^+$CD3$^-$ cells' *in vivo* function in pathogenesis, 2×10^6 purified PBMC CD8αα$^+$CD3$^-$ cells of immunized LEW rats were injected into WKY rats at 17 days post immunization. Cell transfer was repeated at day 20 and 25. As a control, immunized rats received the same number of PBMC CD8α$^-$ cells. Severity of glomerulonephritis in the cell recipients were examined at day 45. In some cases, GIL CD8αα$^+$ cells were isolated from the cell recipients at d25. Genomic DNA was isolated from the cells for genotyping using three polymorphic DNA microsatellites following an established method.[15] The renal tissues were also used for detection of apoptotic cells and infiltration of GIL CD8αα$^+$ cells. Data represent one experiment of two separate experiments (three rats/group). Control GIL CD8αα$^+$ cells were isolated following a previously published method.

Stimulation of PBMC CD8αα$^+$CD3$^-$ cell by LPS

A published protocol for macrophages was followed for stimulation of PBMC CD8αα$^+$CD3$^-$ cells with LPS with minor modifications.[37] Briefly, the purified CD8αα$^+$CD3$^-$ cells were adjusted to 10^6 cells/ml with complete DMEM medium containing 5% fetal calf serum and 0.5 ml of cell suspension was added to each well of 24-well plate, or chamber slide. The plate was incubated for overnight for the cells to adhere. Supernatant in each well was then replaced with fresh medium. One μl of E *coli* LPS (5 μg/ml, Sigma, St Louis) was added to each well. After incubation for 2 hrs at 37°C, LPS was removed by repeated replacements of supernatant. Golgi stop reagent (GolgiStop™, BD Biosciences, San Diego, CA) was immediately added to the wells of chamber slide. The cells were fixed and permeablized after 6 hrs and used for detection of intracellular RT1D by immunofluorescence. Cells in the 24-well plate were harvested by repeated pipetting after incubation for 1, 2 or 3 days. The harvested cells were immediately stained with FITC-labeled antibody to RT1D for measuring their cell surface RT1D by flow cytometry.

Statistical analysis

T-tests were performed for comparison between various experimental results such as GIS. The χ^2 test was used for the distribution of labeled cells in glomeruli. p value < 0.05 was considered significant.

ACKNOWLEDGEMENTS

This study was supported by NIH R01-DK60029 and R01-DK077857 (Y.H.L.). J.R. was supported by NIH T32-DE015355. Histology support was provided by the Pathology Laboratory, University of Texas HSC at Houston.

REFERENCES

1. Salama AD, Levy JB, Lightstone L, et al. Goodpasture's disease. Lancet. 2001; 358:917–920. [PubMed: 11567730]
2. Waldmann TA. Immunotherapy: past, present, and future. Nat Med. 2003; 9:269–277. [PubMed: 12612576]
3. Morgan RA, Dudley ME, Wunderlich JR, et al. Cancer regression in patients after transfer of genetically engineered lymphocytes. Science. 2006; 314:126–129. [PubMed: 16946036]
4. Rotrosen D, Matthews JB, Bluestone JA. The immune tolerance network: a new paradigm for developing tolerance-inducing therapies. J Allergy Clin Immunol. 2002; 110:17–23. [PubMed: 12110811]
5. Hilkens CM, Isaacs JD, Thomson AW. Development of dendritic cell-based immunotherapy for autoimmunity. Int Rev Immunol. 2010; 29:156–183. [PubMed: 20199240]
6. O'Brien KB, Gran B, Rostami A. T-cell based immunotherapy in experimental autoimmune encephalomyelitis and multiple sclerosis. Immunotherapy. 2010; 2:99–115. [PubMed: 20231863]
7. Chorny A, Gonzalez-Rey E, Fernandez-Martin A, et al. Vasoactive intestinal peptide induces regulatory dendritic cells with therapeutic effects on autoimmune disorders. Proc Natl Acad Sci USA. 2005; 102:13562–13567. [PubMed: 16150720]
8. Mekala DJ, Geiger TL. Immunotherapy of autoimmune encephalomyelitis with redirected $CD4^+CD25^+$ T lymphocytes. Blood. 2005; 105:2090–2092. [PubMed: 15528313]
9. Kamath AT, Sheasby CE, Tough DF. Dendritic cells and NK cells stimulate bystander T cell activation in response to TLR agonists through secretion of IFN-α and IFN-γ. J Immunol. 2005; 174:767–776. [PubMed: 15634897]
10. Wucherpfennig KW, Strominger JL. Molecular mimicry in T cell-mediated autoimmunity: viral peptides activate human T cell clones specific for myelin basic protein. Cell. 1995; 80:695–705. [PubMed: 7534214]
11. Wu J, Hicks J, Ou C, et al. Glomerulonephritis induced by recombinant Col4α3NC1 is not associated with antibody to GBM: a potential T cell mediated mechanism. J Immunol. 2001; 167:2388–2395. [PubMed: 11490029]
12. Wu J, Hicks J, Borillo J, et al. $CD4^+$ T cells specific to glomerular basement membrane antigen induce glomerulonephritis . J Clin Invest. 2002; 109:517–524. [PubMed: 11854324]
13. Wu J, Borillo J, Glass WF II, et al. T cell epitope of glomerular basement membrane antigen induces severe glomerulonephritis. Kidney Intl. 2003; 64:1292–1301.
14. Robertson J, Wu J, Arends J, et al. Spontaneous recovery from early glomerular inflammation is associated with resistance to anti-GBM glomerulonephritis: tolerance and autoimmune tissue injury . J Autoimmunity. 2008; 30:246–256. [PubMed: 18054199]
15. Wu J, Zhou C, Robertson J, et al. Identification of a bone marrow derived $CD8\alpha\alpha^+$ dendritic cell like population in inflamed autoimmune target tissue with capability of inducing T cell apoptosis. J Leukoc Biol. 2010; 88:831–835. [PubMed: 21041514]
16. Zhou C, Wu J, Robertson J, et al. Natural recovery from anti-GBM glomerulonephritis is associated with glomeruli-infiltrating $CD8\alpha^+CD11c^+$MHC class-II^+ cells. Am J Nephrol. 2011; 34:519–528. [PubMed: 22068125]
17. Wang YM, Zhang GY, Hu M, et al. $CD8^+$ regulatory T cells induced by T cell vaccination protect against autoimmune nephritis. J Am Soc Nephrol. 2012; 23:1058–1067. [PubMed: 22491420]
18. Brenan M, Puklavec M. The MRC OX-62 antigen: a useful marker in the purification of rat veiled cells with the biochemical properties of an integrin. J Exp Med. 1992; 175:1457–1465. [PubMed: 1588275]
19. Steinman RM, Idoyaga J. Features of the dendritic cell lineage. Immunol Rev. 2010; 34:5–17. [PubMed: 20193008]
20. Steinman RM, Hawiger D, Nussenzweig MC. Tolerogenic dendritic cells. Ann Rev Immunol. 2003; 21:685–711. [PubMed: 12615891]

21. Trinite B, Chauvin C, Peche H, et al. Immature CD4-CD103^{+} rat dendritic cells induce rapid caspase-independent apoptosis-like cell death in various tumor and nontumor cells and phagocytose their victims. J Immunol. 2005; 175:2408–2417. [PubMed: 16081812]
22. Suss G, Shortman KA. A subclass of dendritic cells kills CD4 T cells via Fas/Fasligand- induced apoptosis. J Exp Med. 1996; 183:1789–1796. [PubMed: 8666935]
23. John R, Nelson PJ. Dendritic cells in the kidney. J Am Soc Nephrol. 2006; 18:2628–2635. [PubMed: 17804672]
24. Velazquez P, Dustin ML, Nelson PJ. Renal dendritic cells: an update. Nephron Exp Nephrol. 2009; 111:e67–e71. [PubMed: 19276627]
25. Soos TJ, Sims TN, Barisoni L, et al. CX3CR1^{+} interstitial dendritic cells form a contiguous network throughout the entire kidney. Kidney Int. 2006; 70:591–596. [PubMed: 16760907]
26. Hochheiser K, Tittel A, Kurts C. Kidney dendritic cells in acute and chronic disease. Int J Exp Pathol. 2010 Doi: 10.1111.
27. Kruger T, Benke D, Eitner F, et al. Identification and functional characterization of dendritic cells in the healthy murine kidney and in experimental glomerulonephritis. J Am Soc Nephrol. 2004; 15:613–621. [PubMed: 14978163]
28. Heymann F, Meyer-Schwesinger C, Hamilton-Williams EE, et al. Kidney dendritic cell activation is required for progression of renal disease in a mouse model of glomerular injury. J Clin Invest. 2009; 119:1286–1297. [PubMed: 19381017]
29. Georgiev M, Agle LM, Chu JL, et al. Mature dendritic cells readily break tolerance in normal mice but do not lead to disease expression. Arthritis Rheum. 2005; 52:225–238. [PubMed: 15641101]
30. Wan S, Xia C, Morel L. IL-6 produced by dendritic cells from lupus-prone mice inhibits CD4^{+}CD25^{+} T cell regulatory functions. J Immunol. 2007; 178:271–279. [PubMed: 17182564]
31. Reynolds J, Norgan VA, Bhambra U, et al. Anti-CD8 monoclonal antibody therapy is effective in the prevention and treatment of experimental autoimmune glomerulonephritis. J Am Soc Nephrol. 2002; 13:359–369. [PubMed: 11805163]
32. Sung SJ, Bolton WK. Are men rats? dendritic cells in autoimmune glomerulonephritis. J Leukoc Biol. 2010; 88:831–835. [PubMed: 21041514]
33. Poulin LF, Salio M, Griessinger E, et al. Characterization of human DNGR-1^{+} BDCA3^{+} leukocytes as putative equivalents of mouse CD8α^{+} dendritic cells. J Exp Med. 2010; 207:1261–1271. [PubMed: 20479117]
34. Mesnard L, Keller ADC, Michel ML, et al. Invariant natural killer T cells and TGF-β attenuate anti-GBM glomerulonephritis. J Am Soc Nephrol. 2009; 20:1282–1292. [PubMed: 19470687]
35. Wolf D, Hochegger K, Wolf AM, et al. CD4^{+}CD25^{+} regulatory T cells inhibit experimental anti–Glomerular basement membrane glomerulonephritis in mice. J Am Soc Nephrol. 2005; 16:1360–1370. [PubMed: 15788479]
36. Aitman TJ, Dong D, Vyse TJ, et al. Copy number polymorphism in Fcgr3 predisposes to glomerulonephritis in rats and humans. Nature. 2006; 439:851–855. [PubMed: 16482158]
37. Fortier, AH. Activation of murine macrophages. In: Coligan, JE.; Kruisbeek, AM.; Margulies, DH., et al., editors. Current Protocols in Immunology. Vol. 3. John Willey & Sons; 1991. p. 14.4.1-14.4.5.

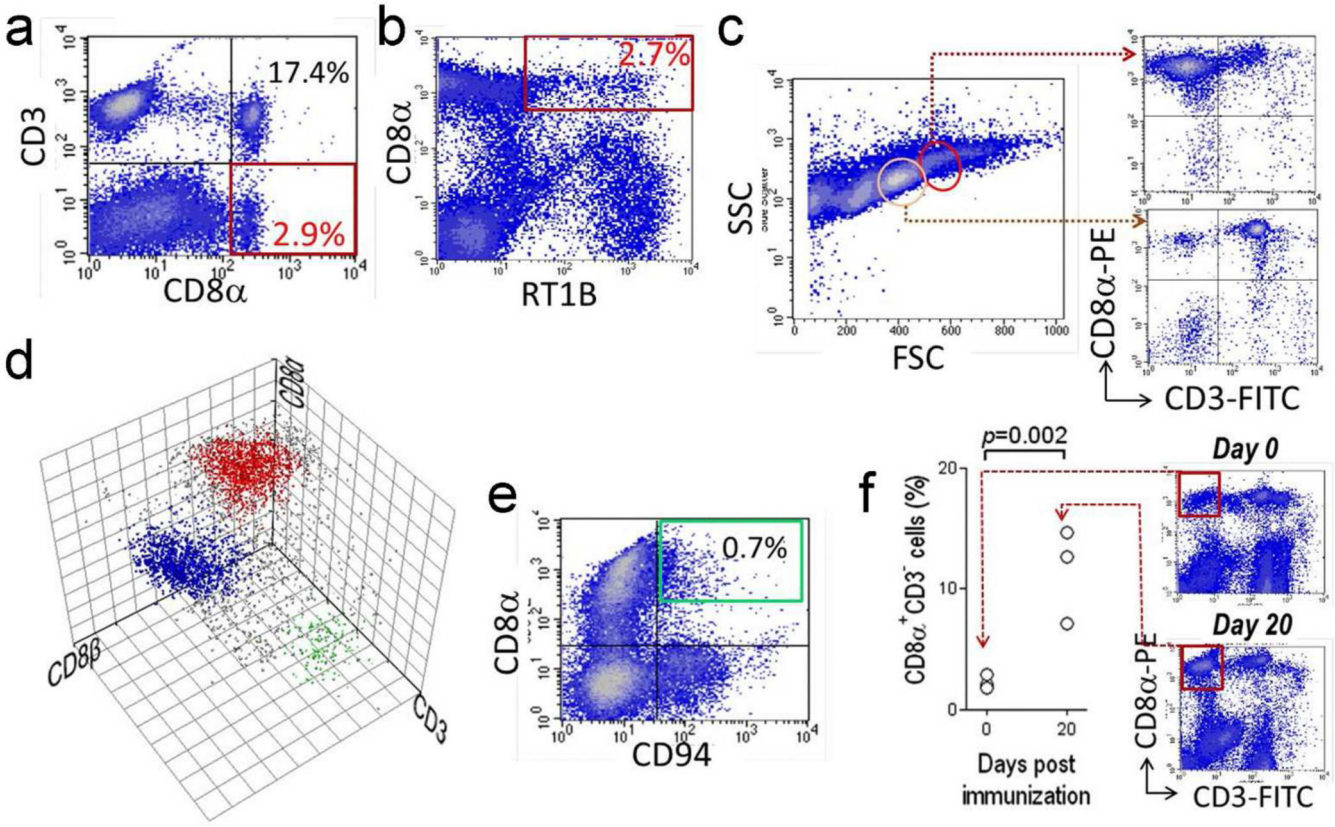

Figure 1. Identification of PBMC CD8α$^+$β$^-$RT1B(MHC-II)$^+$CD3$^-$ population and its expansion after immunization

(**a** and **b**) Flow cytometry analyses on PBMC show a CD8α$^+$CD3$^-$ population (red box in **a**) and a CD8α$^+$RT1B$^+$ population (red box in **b**). (**c**) FSC/SSC plot analysis of sorted PBMC CD8α$^+$ cells shows two morphologically distinct populations (red and pink circle), which were CD8α$^+$CD3$^-$ (right upper panel) and CD8α$^+$CD3$^+$ T cells (right lower panel), respectively. (**d**) Three color flow cytometry shows distinct populations of CD8α$^+$β$^-$CD3$^-$ cells (red dots) and CD8α$^+$β$^+$CD3$^+$ T cells (blue dots) among sorted PBMC CD8α$^+$ cells. A small CD8$^-$CD3$^+$ T cell population (green dots), probably CD4$^+$ T cell contaminant, also can be seen. (**e**) Flow cytometry on PBMC shows a majority population of CD8α$^-$CD94$^+$ NK cells and a minor CD8α$^+$CD94$^+$ population (green box). (**f**) Expansion of the PBMC CD8α$^+$CD3$^-$ population after immunization (left panel)(*n*=3 for normal and immunized group). Right two panels are representative flow cytometries on PBMC at d0 and d20 post immunization with pCol(28–40) for comparison of CD8α$^+$CD3$^-$ populations (red box).

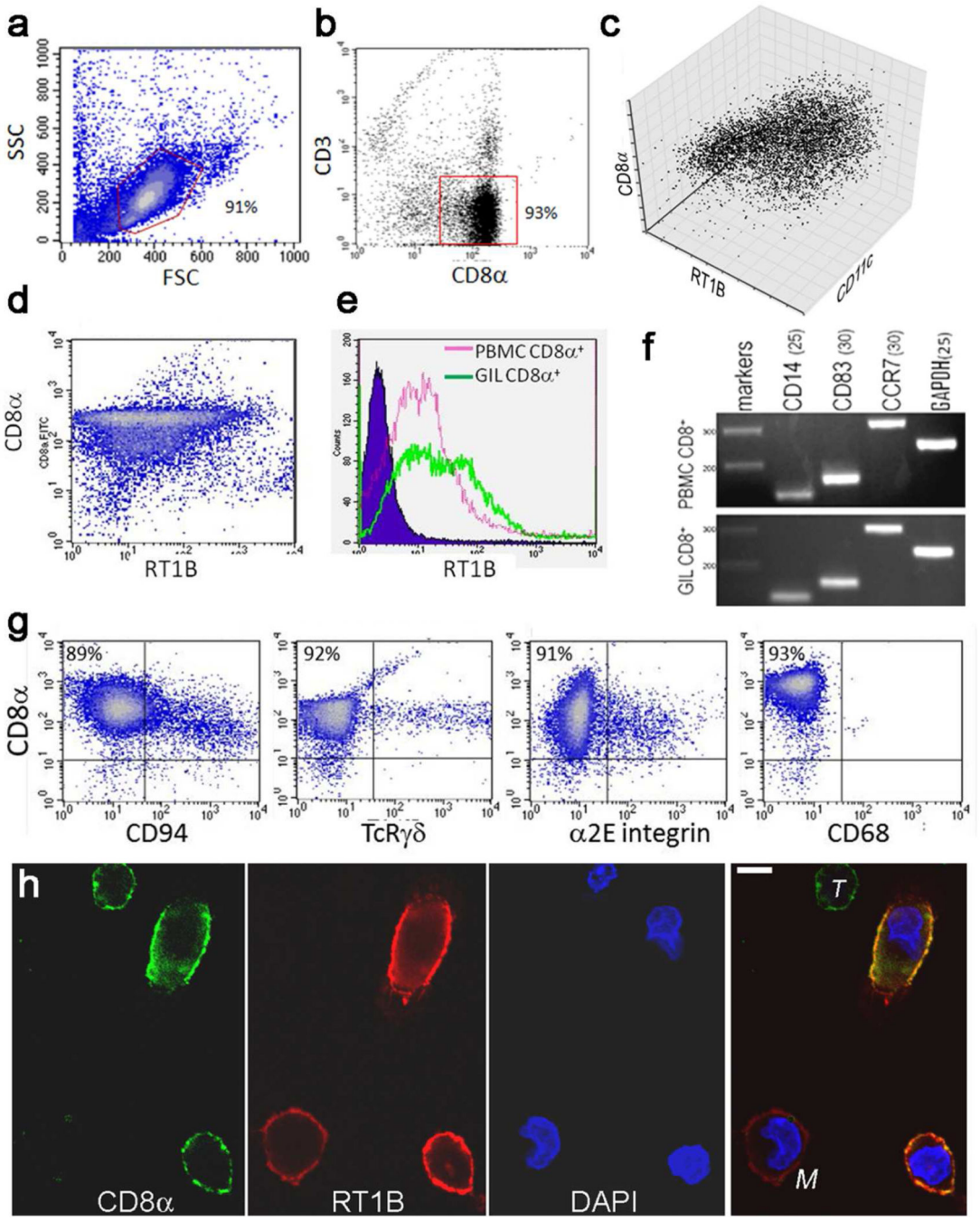

Figure 2. Characterization of purified PBMC CD8αα$^+$CD3$^-$ cells

(**a** and **b**) The purified PBMC CD8αα$^+$ cells form a morphologically distinct population (red gate in **a**) with a phenotype of CD8α$^+$CD3$^-$ (red box in **b**). (**c**) Three-color flow cytometry shows the purified cells to be CD8α$^+$CD11c$^+$RT1B(MHC II)$^+$. (**d**) The PBMC CD8αα$^+$CD3$^-$ cells express various levels of RT1B. (**e**) A histogram plot compares RT1B expression levels between purified PBMC CD8αα$^+$CD3$^-$ cells and GIL CD8αα$^+$ cells; isotype control is shown as blue line. (**f**) RT-PCR detection of expression of various markers as indicated, in comparison to those for GIL CD8αα$^+$ cells; DNA size markers are shown at

the left. Cycles for PCR are indicated within parentheses. (**g**) The PBMC CD8αα$^+$ cells are negative for CD94, TcRγδ, α2E integrin, and CD68 (ED1). (**h**) Immunofluorescences show the morphology of PBMC CD8αα$^+$ cells in comparison to PBMC monocytes (*M*) or CD8$^+$ T cells (*T*) after staining for CD8α (green) and RT1B (red). Note characteristic kidney-shaped nucleus in monocyte after DAPI counter-staining. X400, Bar = 10 μm.

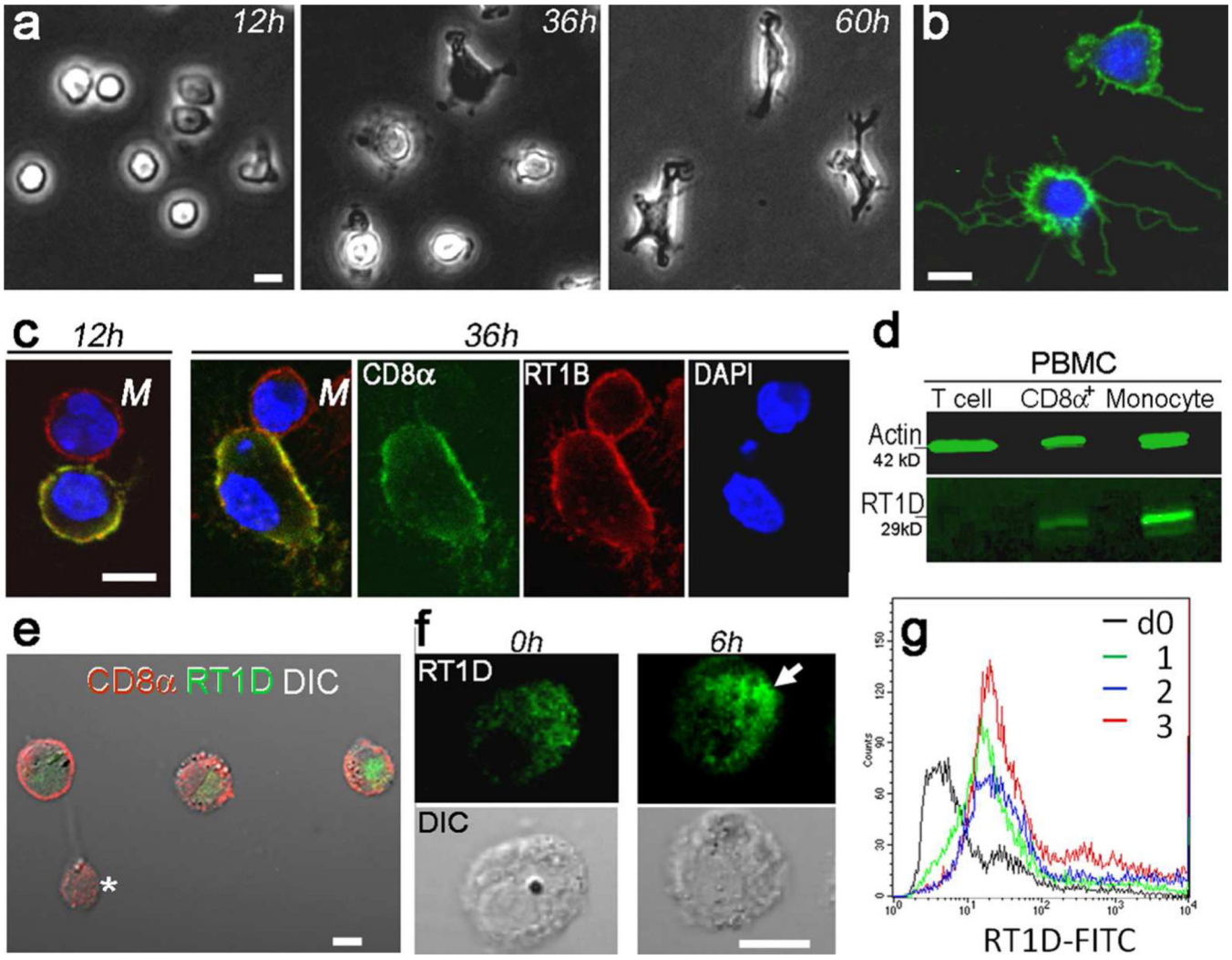

Figure 3. Spontaneous differentiation of PBMC CD8αα^{+}CD3^{-} cells into DC-like cells after a short-term *in vitro* culture

(**a**) Phase-contrast micrographs show morphological changes in purified PBMC CD8αα^{+}CD3^{-} cells after culture as indicated. (**b**) Anti-CD8α antibody reveals dendrite-like cellular projections of PBMC CD8αα^{+}CD3^{-} cells after a 3-day culture. (**c**) Comparison of morphological changes between PBMC CD8αα^{+}CD3^{-} cells (red and green) and PBMC CD8αα^{-}RT1B^{+} monocytes (M)(red); PBMC CD8αα^{+}CD3^{-} cells become flattened at 36hr, while a nearby monocyte remains spherical shaped. (**d**) Western blot shows expression of MHC II (RT1D) in PBMC CD8αα^{+}CD3^{-} cells in comparison to monocytes. (**e**) Intracellular RT1D (green) was demonstrated by confocal immunofluorescence after permeablization of the cells; the cells were co-stained for CD8α (red). A CD8^{+} T cell (asterisk) is shown as a negative control for RT1D staining. (**f**) Active synthesis of RT1D was detected by comparison between the cells before (0hr) and after Golgi blockage (6hr); an arrow shows an accumulation of RT1D in the cell. DIC, differential interference contrast. (**g**) Up-regulation of surface RT1D expression in PBMC CD8αα^{+}CD3^{-} cells after incubation with LPS as indicated. Bars = 10 μm.

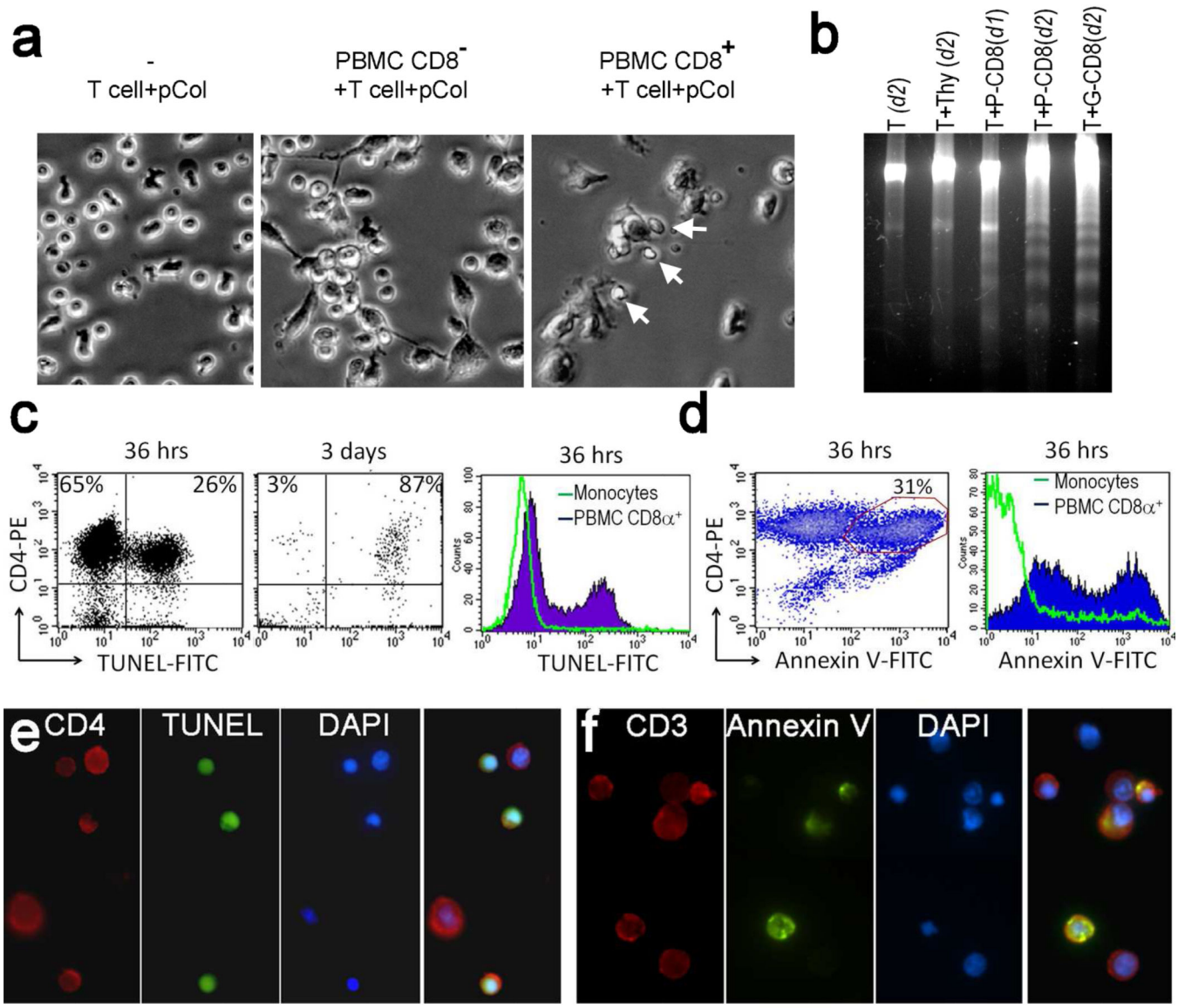

Figure 4. PBMC CD8αα$^+$CD3$^-$ cells induce T cell apoptosis *in vitro*

(**a**) Phase contrast micrographs show cells in the incubations under indicated conditions at d3. Arrows indicate cell debris. (**b**) DNA fragmentation in the cells from various incubations as indicated at the top of each lane at d1 or d2. *P-CD8*, PMBC CD8αα$^+$CD3$^-$ cells; *G-CD8*, GIL CD8αα$^+$ cells; *Thy*, thymocytes; *T*, T cells. (**c**) TUNEL detection of apoptotic CD4$^+$ cells at different time points post incubation with PMBC CD8αα$^+$CD3$^-$ cells; histogram at right is comparison of TUNEL$^+$CD4$^+$ population between incubations with CD8α$^-$ monocytes and PBMC CD8αα$^+$CD3$^-$ cells. (**d**) Detection of T cell apoptosis after incubation with PBMC CD8αα$^+$CD3$^-$ cells using a combination of annexin V and CD4 Ab; the annexin V$^+$CD4$^+$ population is highlighted by a red gate; the histogram at the right is a comparison of annexin$^+$ cells among CD4$^+$ T cells after incubation with monocytes or PMBC CD8αα$^+$CD3$^-$ cells. (**e**) Immunofluorescence shows co-localization of surface CD4

(red) with nuclear TUNEL (green). (**f**) Immunofluorescence demonstrates cell surface CD3 (red) and annexin V (red). Notice abnormal nuclei in apoptotic T cells. Bars = 20 μm.

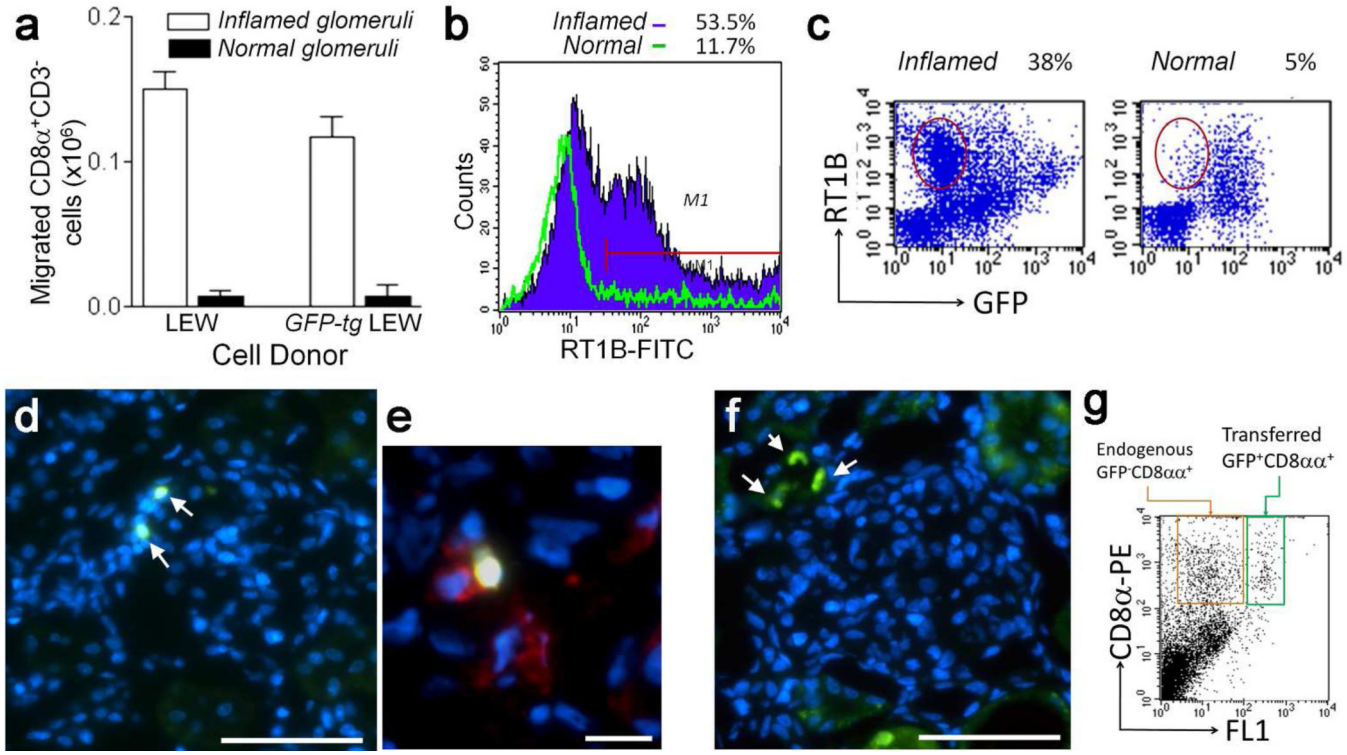

Figure 5. PBMC CD8αα$^+$CD3$^-$ cells are able to migrate toward or infiltrate inflamed glomeruli

(**a**) Summary of *in vitro* migration assays using CFSE-labeled PBMC CD8α$^+$CD3$^-$ cells from immunized LEW rats (CFSE$^+$) or those from immunized LEW GFP-Tg rats; migrated cells were those found in the lower chamber. (**b**) Histogram analysis of the migrated cells for their RT1B expression when whole PBMC CD8$^+$ cells (including CD3$^+$ and CD3$^-$ populations) of LEW rats were labeled and used as probes. Note that most PBMC CD8$^+$ cells which had migrated toward inflamed glomeruli were RT1B$^+$. (**c**) Analyses of migrated cells when whole PBMC CD8α$^+$ cells of LEW GFP-Tg rats were used as probes; normal or inflamed glomeruli of WKY rats were used as chemoattractants as indicated; percentages of migrated GFP$^+$RT1B$^+$ cells (red circle) to whole GFP$^+$CD8$^+$ population are indicated at the top of each plot. Other two experiments showed similar results. Note that RT1B$^+$ cells had a lower GFP level than other cells as expected. (**d**) Fluorescent micrograph reveals two transferred CFSE$^+$CD8α$^+$ cells (arrows) in a glomerulus of an immunized WKY recipient. Bar = 50 μm. (**e**) Immunofluorescence shows a transferred CFSE$^+$ PBMC CD8αα$^+$CD3$^-$ (arrow) with endogenous GIL CD8αα$^+$ cells (red). Bar = 15 μm. (**f**) Three transferred GFP$^+$ PBMC CD8αα$^+$CD3$^-$ cells (arrows) are in Bowman's capsule of a glomerulus of an immunized WKY recipient. Bar = 50 μm. (**g**) Flow cytometry shows a GFP$^+$CD8α$^+$ population (green gate) among glomerular cells isolated from immunized WKY rats that had been injected with GFP$^+$ PBMC CD8αα$^+$CD3$^-$ cells.

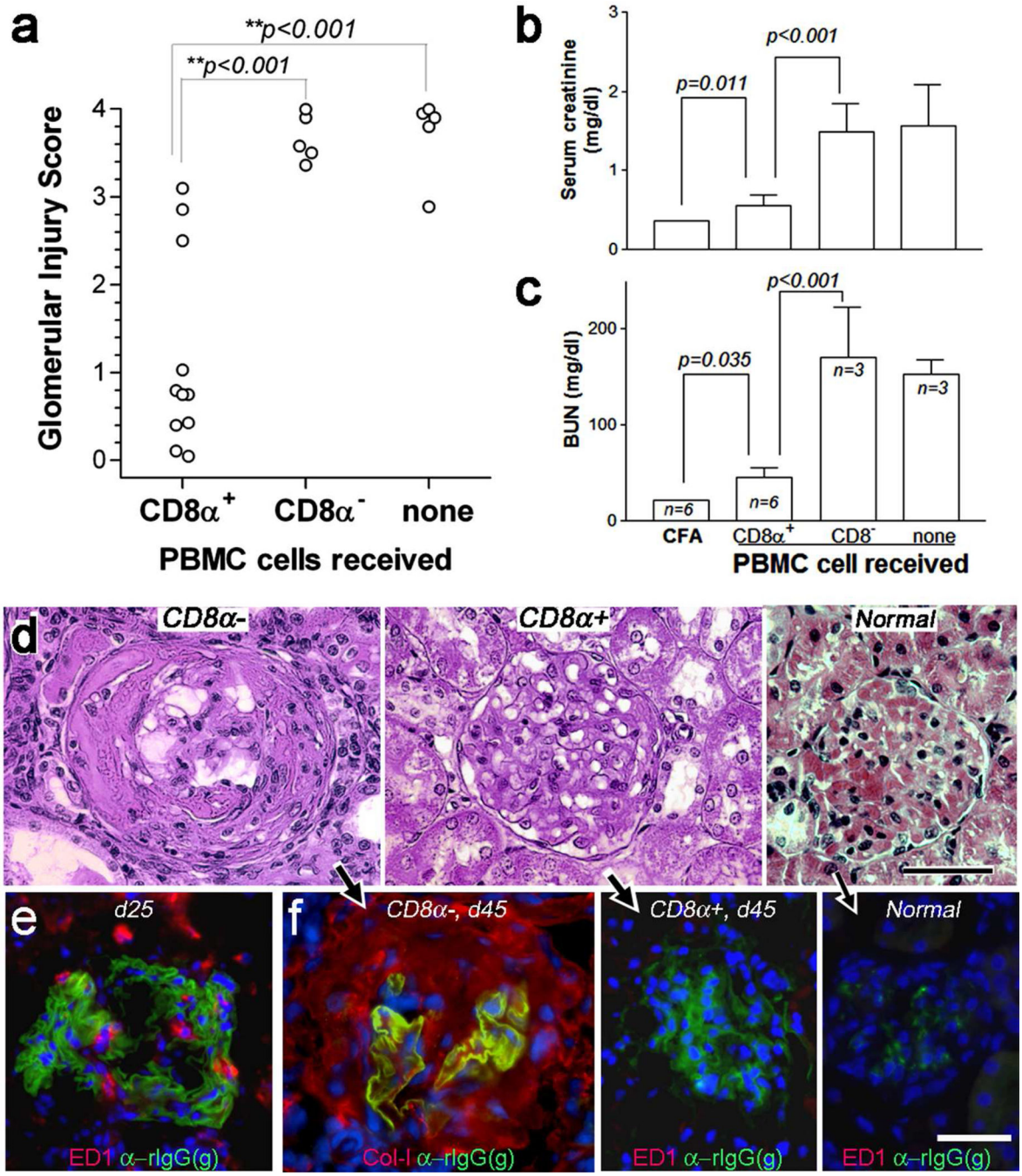

Figure 6. Transfer of PBMC CD8αα^{+}CD3^{-} cells of GN-resistant LEW rats attenuates GN in WKY recipient rats

(**a**) Summary of GN severities in immunized WKY rats which had received PBMC CD8αα^{+}CD3^{-} cells (CD8α^{+}) or PBMC CD8^{-} cells (CD8^{-}) of LEW rats, or did not receive any cells (none). (**b, c**) Serum creatinine (**b**) and BUN (**c**) in different experimental groups as indicated. (**d**) Representative histology shows glomeruli from WKY rats as indicated (CD8α^{-} = PBMC CD8α^{-} recipient; CD8α^{+} = PBMC CD8αα^{+}CD3^{-} recipient) at d45. Note a circumferential fibrous crescent in PBMC CD8α^{-} recipient. Also note that the glomerulus

is slightly dilated without any inflammation in PBMC CD8αα^{+}CD3^{-} recipient as compared to normal glomeruli. (**e**) Immunofluorescence shows presence of ED1^{+} macrophages (red) and GBM-bound IgG (green) in the immunized WKY rats at d25. (**f**) Immunofluorescent micrographs from the same animals in **d** (connected by arrows) show staining for either ED1^{+} macrophage (red) or collagen I (Col-I, red) in addition to GBM-bound IgG (green). Note that collagen I staining reveals a fibrous crescent (red) surrounding collapsed tuft (green) in a PBMC CD8α^{-} recipient WKY. Also note that a glomerulus from PBMC CD8αα^{+}CD3^{-} recipient WKY shows weak positive for GBM-bound IgG but no ED1^{+} macrophages. Bar = 50 μm

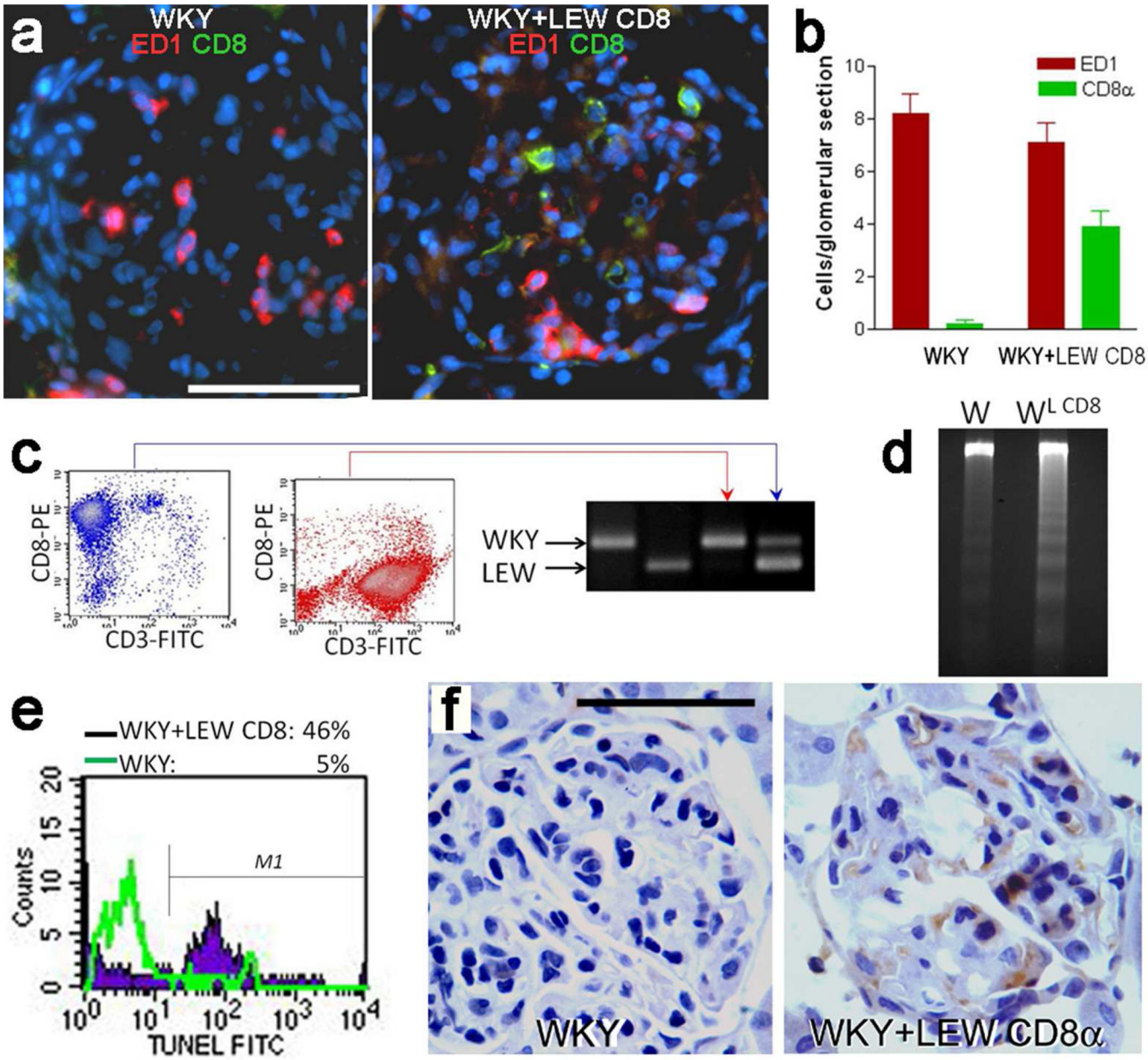

Figure 7. Increased GIL CD8αα$^+$ cells and T cell apoptosis in the glomeruli of PBMC CD8αα$^+$CD3$^-$ recipient WKY rats at d23

(**a**) Immunofluorescence shows increased CD8α$^+$ cells (green) in a glomerulus of a PBMC CD8αα$^+$CD3$^+$ cell-recipient WKY rat (WKY-LEW CD8) as compared to immunized WKY (WKY) at d23 (*n*=3). (**b**) Summary of CD8α$^+$ cells and ED1$^+$ macrophages in the glomeruli in experimental groups as indicated. (**c**) Genotyping of glumeruli-infiltrating cells using DNA microsatellite based PCR. Pooled GIL CD8αα$^+$ cells (shown as CD8α$^+$CD3$^-$, left panel) and CD3$^+$ pan T cells (second to the left) pooled from three PBMC CD8αα$^+$CD3$^+$ cell-recipient WKY rats. The right panel shows PCR products with primers for microsatellite (D7R24). Note that GIL CD8αα$^+$ cells are predominantly LEW type while T cells are absolutely WKY type. (**d**) DNA fragmentation assay for the pan T cells (refer to **c**)

isolated from the glomeruli of immunized WKY rats (W) or PBMC CD8αα^{+}CD3^{+} cell-recipient WKY rats (W^{LCD8}). The T cells were incubated for one day before the assay. (**e**) Histogram shows comparison of TUNEL^{+} population among T cells isolated from glomeruli of indicated rats. (**f**) Immunoperoxidase staining for caspase 3 in immunized WKY which received no cells (WKY) or PBMC CD8αα^{+}CD3^{-} cells (WKY+CD8α^{+}). Clustered caspase 3^{+} cells in glomeruli are present in PBMC CD8αα^{+}CD3^{-} cell-recipient WKY rat. Bars = 50 μm.

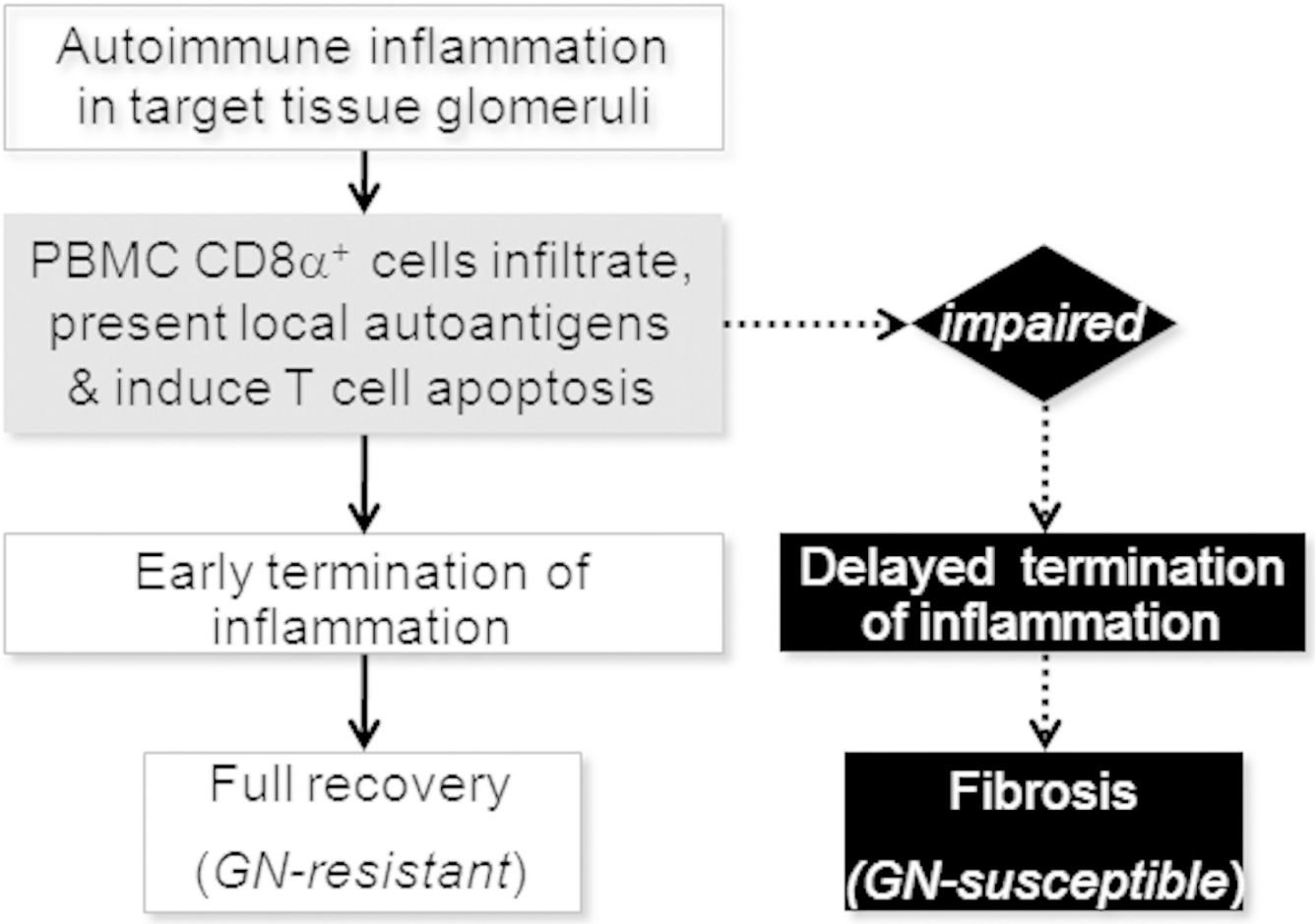

Figure 8. Diagram shows the mechanism, by which a novel PBMC CD8αα^{+}CD3^{-} population terminates autoimmune inflammation in the target tissue glomeruli

Early termination of inflammation leads to a full recovery as seen in GN-resistant LEW rats; delayed termination results in severe fibrosis as seen in GN-susceptible WKY rats.

Table 1

Comparison of phenotypes between PBMC CD8αα^{+}CD3^{-} and GIL CD8αα^{+}cells

	marker	PBL CD8αα^{+}CD3^{-}	GIL CD8αα^{-}
Flow cytometry or immune staining	CD8α	+	+
	CD8β	−	−
	CD3	−	−
	TcRγδ	−	−
	CD68	−	−
	CD94	−	−
	CD11b/c	mid	mid-high
	CD11c	low-mid	mid-high
	RT1B	low-mid	mid-high
	RT1D	low	mid-high
	CD34	low	subset
	TLR3	−	−
	OX40L	−	−
	OX62	−	−
	rNK 1	−	−
RT-PCR	CD14	+	+
	CD83	low	low
	CCR7	mid	mid
	NKG2D	−	−

Table 2

Tissue distribution of transferred CFSE labeled PBMC CD8αα^{+}CD3^{-} cells in the kidneys of recipient WKY rats

	Observed	Expected based on the areas
Glomerular	82 (60.7%)	10.6%
Interstitial	53 (39.3%)	89.4%
	135 (100.0%)	100.0%

[1] χ^2=358.2, two-tailed p<0.0001

[2] This is a representative result from one of three recipients. Similar results were observed in the other two.